Ground state and elementary excitations of single and binary Bose-Einstein condensates of trapped dipolar gases

K. Góral[1,2] and L. Santos[1]

[1]*Institut für Theoretische Physik, Universität Hannover, D-30167 Hannover, Germany*
[2]*Center for Theoretical Physics, Polish Academy of Sciences, Aleja Lotników 32/46, 02-668 Warsaw, Poland*

We analyze the ground-state properties and the excitation spectrum of Bose-Einstein condensates of trapped dipolar particles. First, we consider the case of a single-component polarized dipolar gas. For this case we discuss the influence of the trapping geometry on the stability of the condensate as well as the effects of the dipole-dipole interaction on the excitation spectrum. We discuss also the ground state and excitations of a gas composed of two antiparallel dipolar components.

I. INTRODUCTION

The nature and stability of a Bose-Einstein condensate (BEC) [1,2] are strongly influenced by the interparticle interactions that are described by the s-wave scattering length a. If $a > 0$ the interactions are repulsive, and condensates with an arbitrary large number of particles are stable. On the contrary, spatially homogeneous condensates with $a < 0$ are absolutely unstable with regard to local collapses [3]. The presence of a trapping potential changes the situation drastically, as revealed in successful experiments with magnetically trapped atomic ^{7}Li ($a = -14$ Å) [2,4]. As found in theoretical studies [5–7], there will be a metastable BEC if the number of condensed particles is sufficiently small, such that the spacing between the trap levels exceeds the mean-field interparticle interaction $n_0|g|$ (where n_0 is the condensate density, $g = 4\pi\hbar^2 a/m$, and m is the atom mass). In other words, the BEC is stabilized if the negative pressure caused by the interparticle attraction is compensated by the quantum pressure imposed by the trapping potential.

The effects of the interparticle interactions on the condensate properties have been mainly discussed for the case of van der Waals (short-range) interactions. However, the BEC in the presence of dipole-dipole interactions has recently raised a considerable interest [8–16]. Novel physics is expected for dipolar BEC, since the dipole-dipole interactions are long range, anisotropic, and partially attractive. The nontrivial task of achieving and controlling dipolar BECs is thus particularly challenging.

The interest in dipolar gases has been partially motivated by the recent success in creating ultracold molecular clouds [17,18]. This success opens fascinating prospects to achieve quantum degeneracy in trapped gases of heteronuclear molecules that could interact via electric dipole-dipole forces after being oriented in a sufficiently high electric field. On the other hand, the ultracold gases of atoms with large magnetic dipole moments, such as chromium [19–23] or europium [24], have also been a subject of growing interest. In this case, the dipole-dipole interactions are not expected to be dominant, although for a relatively small a the BEC may reflect the interplay between short-range and dipole-dipole interactions [9,13]. Interestingly, these effects can be ampli-

fied by reducing a via Feshbach resonances [25,26]. Similar effects have been discussed in Refs. [8,11,12] for ground-state atoms with electric dipole moments induced by high dc electric fields (of the order of 10^6 V/cm). It has been also suggested that laser-induced dipole-dipole interactions could be achieved by exciting atoms to Rydberg states [10]. In this case applications to quantum information processing have been discussed (see, e.g., Ref. [27]).

The stability of the condensate is significantly modified by the presence of dipole-dipole interactions [8–11,13]. In particular, a BEC of particles dominantly interacting via dipole forces is, similar to condensates with $a < 0$, unstable in a spatially homogeneous case and can be stabilized by confinement in a trap. It has been shown [10] that the sign and the value of the dipole-dipole interaction energy is strongly influenced by the trapping geometry and, hence, the stability diagram depends crucially on the trap anisotropy. This opens new, interesting possibilities for controlling and engineering macroscopic quantum states. In particular, for dipoles oriented along the axis of a cylindrical trap there exists a critical value $l^* = 0.4$ for the square root of the ratio of the radial to axial frequency $l = (\omega_\rho/\omega_z)^{1/2}$. Pancake traps with $l < l^*$ provide mostly a repulsive mean field of the dipole-dipole interaction, and thus the dipolar condensate in such traps will be stable at any number of particles N. For $l > l^*$ the stability requires $N < N_c$, where the critical value N_c at which the collapse occurs is determined by the condition that (on average) the mean-field interaction energy is attractive and close in absolute value to $\hbar\omega_\rho$.

The study of the condensate properties would be incomplete without the analysis of the excitation spectrum, which determines the dynamical behavior of the system in the regime of weak perturbations. Zero-temperature excitation frequencies have been extensively studied in the case of condensates in dilute alkali gases, both experimentally [28,29] and theoretically [30–32]. In this paper we discuss the low-lying collective excitation frequencies of trapped dipolar BECs, complementing the analysis of Refs. [11,12]. We first consider the case of dominant dipole-dipole interactions, and later on we discuss the situation where the short-range interaction is also relevant. In particular, we discuss in detail the nature of instability and demonstrate that one of the excita-

tions frequencies tends to zero at the criticality as a power of $(N_c-N)^\beta$. We discuss the qualitative character of the low-lying modes, and show that the exponent β undergoes a crossover from 1/4 for $l\gg l^*$ to 2 at $l\simeq l^*$. To illustrate the case of mixed short-range and dipole-dipole interactions, we present predictions for the excitation frequencies for the particular case of a chromium gas.

The second part of the paper is devoted to the analysis of binary dipolar BECs. In recent years, the development of trapping techniques has allowed for creation of multicomponent condensates, formed by atoms in different internal (electronic) states [33,34]. The physics of multicomponent BEC, far from being a trivial extension of the single-component one, presents novel and fundamentally different scenarios for its ground-state wave function [35,36] and excitations [37]. In particular, it has been experimentally observed that a BEC can reach an equilibrium state characterized by phase separation of the species in different domains [34]. The analysis of multicomponent BEC has been so far mostly limited to the case of short-range interparticle interactions (a model long-range interaction has been considered in Ref. [36]). One of the main goals of this paper is to analyze the properties of multicomponent dipolar BEC. Such a mixture can be achieved in different physical contexts. In particular, it would be, in general, the case for experiments in ultracold polar molecules [38,41], and in chromium [39] in which different magnetic-moment species are simultaneously trapped in an optical dipole trap. It would also be the case of atomic electric dipoles created by laser-induced pumping to two different Rydberg states. Finally, the same situation would appear in condensates of heteronuclear Hund A diatomic molecules, for which the direction of the magnetic moment is correlated (parallel or antiparallel) with the direction of the molecular axis. Thus, if the magnetic moments are oriented in a magnetic field, the electric moments can acquire two possible directions. We show below that a binary dipolar BEC of two antiparallel dipole components differs qualitatively from the case of a short-range interacting binary BEC.

Our paper is organized as follows. In Sec. II we briefly review the ground-state properties of a single-component BEC of trapped dipolar gases [10]. Section III is devoted to the analysis of the excitation spectrum of single-component trapped dipolar condensed gases. Section IV briefly discusses the ballistic expansion of a dipolar BEC. In Sec. V the ground state of a BEC of two different dipolar species is considered. The excitation spectrum for this case is discussed in Sec. VI. We conclude in Sec. VII.

II. GROUND-STATE PROPERTIES OF A SINGLE-COMPONENT DIPOLAR BEC

A. Description of the system

In this section we briefly review the results of Ref. [10]. We consider a condensate of dipolar particles in a cylindrical harmonic trap. In the following we consider the case of electric dipoles, although the same physics is expected for magnetic ones [9]. All dipoles are assumed to be oriented along the trap axis by a sufficiently strong external field. Accord-

ingly, the dipole-dipole interaction potential between two dipoles is given by $V_d(\mathbf{R})=(d^2/R^3)(1-3\cos^2\theta)$, where d characterizes the dipole moment, $\mathbf{R}$ is the vector between the dipoles ($R=|\mathbf{R}|$ being its length), and θ the angle between $\mathbf{R}$ and the dipole orientation. Similarly as in Refs. [8–10], we describe the dynamics of the condensate wave function $\psi(\mathbf{r},t)$ by using the time-dependent Gross-Pitaevskii equation (GPE):

$$i\hbar\frac{\partial}{\partial t}\psi(\mathbf{r},t)=\left\{-\frac{\hbar^2}{2m}\nabla^2+\frac{m}{2}(\omega_\rho^2\rho^2+\omega_z^2z^2)+g|\psi(\mathbf{r},t)|^2\right.$$
$$\left.+d^2\int d\mathbf{r}'\frac{1-3\cos^2\theta}{|\mathbf{r}-\mathbf{r}'|^3}|\psi(\mathbf{r}',t)|^2\right\}\psi(\mathbf{r},t),$$

$$(1)$$

where $\psi(\mathbf{r},t)$ is normalized to the total number of condensate particles N. The third term in the rhs of Eq. (1) corresponds to the mean field of short-range (van der Waals) forces and the last term to the mean field of the dipole-dipole interaction. In this section, we omit the term $g|\psi(\mathbf{r},t)|^2\psi(\mathbf{r},t)$, assuming that the interparticle interaction is dominated by dipole-dipole forces ($d^2\gg|g| =4\pi\hbar^2|a|/m$) and the system is away from shape resonances of $V_d(\mathbf{R})$. The effects of the short-range interactions on the excitation spectrum are discussed in detail in Sec. III.

The wave function of the relative motion of a pair of dipoles is influenced by the dipole-dipole interaction at interparticle distances $|\mathbf{r}-\mathbf{r}'|\lesssim r^*=2md^2/\hbar^2$. This influence is ignored in the dipole-dipole term of Eq. (1), as the main contribution to the integral comes from distances $|\mathbf{r}-\mathbf{r}'|$ of order the spatial size of the condensate, which we assume to be much larger than r^*.

Away from the shape resonances, the dipolar condensate is unstable in the spatially homogeneous case. For all dipoles parallel to each other, by using the Bogoliubov method, one finds an anisotropic dispersion law for elementary excitations: $\varepsilon(\mathbf{k})=[E_k^2+8\pi E_k n_0 d^2(\cos^2\theta_k-1/3)]^{1/2}$, where $E_k =\hbar^2k^2/2m$, n_0 is the condensate density, and θ_k is the angle between the excitation momentum $\mathbf{k}$ and the direction of the dipoles. The instability is clearly seen from the fact that at small k and $\cos^2\theta_k<1/3$, imaginary excitation energies ε emerge.

B. Numerical results

Equation (1), contrary to the usually employed GPE with short-range interactions, is an integro-differential equation. The evaluation of the integral term deserves special attention, since the integrand diverges at relative interparticle distances tending to zero. Fortunately, the calculation of the integral term can be simplified by means of the convolution theorem:

$$d^2\int d\mathbf{r}'\frac{1-3\cos^2\theta}{|\mathbf{r}-\mathbf{r}'|^3}|\psi(\mathbf{r}')|^2=\mathcal{F}^{-1}\{\mathcal{F}[V](\mathbf{q})\mathcal{F}[|\psi|^2](\mathbf{q})\},$$

$$(2)$$

where $\mathcal{F}$ and $\mathcal{F}^{-1}$ indicate the Fourier transform and the

inverse Fourier transform, respectively. The Fourier transform of the dipole-dipole potential reads

$$\mathcal{F}[V](\mathbf{q}) = 4\pi d^2 (1 - 3\cos^2\alpha)\left[\frac{\cos(bq)}{(bq)^2} - \frac{\sin(bq)}{(bq)^3}\right], \tag{3}$$

where α is the angle between the momentum $\mathbf{q}$ and the dipole direction, and b is a cutoff distance corresponding to the atomic radius (a few Bohr radii). Since b is much smaller than any significant length scale of the system, one can safely perform the limit

$$\lim_{b\to 0}\mathcal{F}(V(\mathbf{r})) = \frac{4\pi}{3}d^2(3\cos^2\alpha - 1). \tag{4}$$

In order to evaluate the Fourier transform of Eq. (2), $\mathcal{F}(|\psi|^2)$ is numerically evaluated by means of a standard fast Fourier transform (FFT) algorithm and multiplied by $\mathcal{F}(V(\mathbf{r}))$.

The ground state of the system is obtained by employing a standard split-operator technique in imaginary time. The split-operator technique is also based on a FFT algorithm and, consequently, for each time step four FFTs are needed: two for the calculation of the integral term and two for the evolution. We would like to stress that this procedure constitutes a nontrivial computational task. Additionally, the FFT algorithm must be evaluated in Cartesian coordinates and, as a consequence, computationally demanding fully three-dimensional calculations are required.

To understand the influence of the trapping potential on the dipolar condensate, we have simulated Eq. (1) for various values of the number of particles N, dipole moment d, and the trap aspect ratio l. We have found the conditions under which the condensate is stabilized by the trapping field and investigated static properties of this Bose-condensed state.

For a stationary condensate the wave function $\psi(\mathbf{r},t) = \psi_0(\mathbf{r})\exp(-i\mu t/\hbar)$, where μ is the chemical potential, and the lhs of Eq. (1) becomes $\mu\psi_0(\mathbf{r})$. The important energy scales of the problem are the trap frequencies ω_z, ω_ρ and the dipole-dipole interaction energy per particle defined as $V = (1/N)\int V_d(\mathbf{r}-\mathbf{r}')\psi_0^2(\mathbf{r})\psi_0^2(\mathbf{r}')d\mathbf{r}d\mathbf{r}'$. Accordingly, the trap frequencies, and the (renormalized) number of particles $\sigma = Nr^*/a_{\max}$ [with $a_{\max} = (\hbar/2m\omega_{\min})^{1/2}$ being the maximal oscillator length of the trap] form the necessary set of parameters allowing us to determine the chemical potential and give a full description of the ground state of a trapped dipolar condensate.

We have found that the dipolar condensate is stable either at $V > 0$ or at $V < 0$ with $|V| < \hbar\omega_\rho$. This requires $N < N_c$, where the critical number N_c depends on the trap aspect ratio $l = (\omega_\rho/\omega_z)^{1/2}$. The calculated dependence $N_c(l)$ clearly indicates the presence of a critical point $l^* \simeq 0.43$ [10]. In pancake traps with $l < l^*$, the condensate is stable at any N, because V always remains positive. For small N, the shape of the cloud is Gaussian in all directions. With increasing N, the quantity V increases and the cloud first becomes Thomas-Fermi in the radial direction and then, for a very large N, also axially. The ratio of the axial to radial size of the cloud, L

$= L_z/L_\rho$, continuously decreases with increasing number of particles and reaches a limiting value at $N \to \infty$ (see Fig. 3 of Ref. [10]). In this respect, for a very large N we have a pancake Thomas-Fermi condensate.

For $l \geq 1$, the mean-field dipole-dipole interaction is always attractive. The quantity $|V|$ increases with N and the shape of the cloud changes. In spherical traps the cloud becomes more elongated in the axial direction, and near $N = N_c$ the shape of the cloud is close to Gaussian with the aspect ratio $L = 2.1$. In cigar-shaped traps ($l \gg 1$) especially interesting is the regime where $\hbar\omega_z \ll |V| \ll \hbar\omega_\rho$. In this case the radial shape of the cloud remains the same (Gaussian) as in a noninteracting gas, but the axial behavior of the condensate will be governed by the dipole-dipole interaction which acquires a quasi-one-dimensional (quasi-1D) character. Thus, one has a (quasi) 1D gas with attractive interparticle interactions and is dealing with a stable (bright) solitonlike condensate where attractive forces are compensated by the kinetic energy [41]. L_z decreases with increasing N. Near $N = N_c$, where $|V|$ is close to $\hbar\omega_\rho$, the axial shape of the cloud also becomes Gaussian and the aspect ratio takes the value $L \approx 3.0$. For $l^* \leq l < 1$, the dipole-dipole interaction energy is positive for a small number of particles and increases with N. The quantity V reaches its maximum and further increase in N reduces V and makes the cloud less pancake shaped. At the critical point $N = N_c$ the shape of the cloud is close to Gaussian and the aspect ratio $L < 3.0$.

In the previous analysis, the case of dominant dipole-dipole interactions was considered. However [9,13,8,11], in the general case the effects of the short-range interactions are comparable or even larger than those related to the dipole-dipole interactions. In such situations the short-range term must be maintained in Eq. (1). Provided that a is sufficiently small and positive, the system can become unstable and undergo a collapse in a way similar to what was observed in experiments with ^{7}Li [2] and ^{85}Rb [26]. For the case of negative a, the dipolar gas is expected to be highly unstable, but the dipole-dipole interaction could be employed to stabilize the gas by the trap geometry in a way analogous to the one presented in Ref. [10].

III. EXCITATIONS OF A SINGLE-COMPONENT DIPOLAR BEC

In this section we analyze the collective excitations of a dipolar BEC. Since this is a potentially unstable system, there is a fundamental question about the qualitative and quantitative nature of this instability. Another important question concerns quantitative aspects, in particular how relevant are the effects of the dipole-dipole interaction in the excitation spectrum and to what extent they can observed in the experiments.

In Sec. III A, we briefly summarize the variational approach introduced by Pérez-García et al. [31] and later used by Yi and You [11,12] to describe the low-lying excitation spectrum of a dipolar condensate (for a different variational method using the self-similarity assumption, see Ref. [41]). We employ the notation introduced in Refs. [11,12]. Sec. III B is devoted to the analysis of the behavior of the exci-

tations close to the instability. In Sec. III C, we calculate numerically the response of the system to small perturbations and compare the results with those yielded by the method of Sec. III B. Finally, in Sec. III C, we also discuss how the effects of the dipole-dipole interactions can manifest themselves in the excitation spectrum for various kinds of dipolar gases and trapping geometries.

A. Variational approach

The problem of solving the time-dependent GPE, Eq. (1), can be restated as a variational problem corresponding to the stationary point of the action $S = \int dt d\mathbf{r} \mathcal{L}$ related to the Lagrangian density [11,12,31]:

$$\mathcal{L} = \frac{i}{2} \hbar \left[\psi(\mathbf{r}) \frac{\partial \psi^*(\mathbf{r})}{\partial t} - \psi^*(\mathbf{r}) \frac{\partial \psi(\mathbf{r})}{\partial t} \right] + \frac{\hbar^2}{2m} |\nabla \psi(\mathbf{r})|^2$$

$$+ V_t(\mathbf{r}) |\psi(\mathbf{r})|^2 + \frac{g}{2} |\psi(\mathbf{r})|^4$$

$$+ \frac{u_2}{2} |\psi(\mathbf{r})|^2 \int d\mathbf{r}' \frac{Y_{20}(\theta)}{|\mathbf{r} - \mathbf{r}'|^3} |\psi(\mathbf{r}')|^2, \quad (5)$$

where $u_2 = 4\sqrt{\pi/5} d^2$ and $V_t(\mathbf{r})$ describes the trapping potential. We consider the following Gaussian ansatz for the condensate wave function:

$$\psi(x,y,z,t) = A(t) \prod_{\eta=x,y,z} e^{-\eta^2/2w_\eta^2} e^{i\eta^2 \beta_\eta(t)}, \quad (6)$$

where in contrast to Ref. [11] we omit the possibility of the sloshing motion of the condensate. By inserting the ansatz (6) into Eq. (5) and integrating over the spatial coordinates, one obtains the effective Lagrangian. From this effective Lagrangian one finds the equations of motion of the variational parameters, i.e., the corresponding Euler-Lagrange equations. In particular, if $w_\eta = v_\eta \sqrt{\hbar/m\omega}$, $\omega = \omega_{x,y}$, $\omega_z = \lambda \omega_x$, $v_{x,y} = v$, $P = \sqrt{2/\pi} Na/\sqrt{\hbar/m\omega}$, and $\tau = \omega t$, the Euler-Lagrange equations take the following form:

$$\frac{d^2}{d\tau^2} v_\eta + \lambda_\eta^2 v_\eta = \frac{1}{v_\eta^3} - P \frac{\partial}{\partial v_\eta} \left[\frac{1}{v_x v_y v_z} \left(1 + \frac{u_2}{g} \int d\mathbf{r} \right. \right.$$

$$\left. \left. \times \exp\left(-\sum_\eta \frac{\eta^2}{2v_\eta^2} \right) \frac{Y_{20}(\theta)}{r^3} \right) \right], \quad (7)$$

where $\lambda_{x,y} = 1$ and $\lambda_z = \lambda$. This equation describes the motion of a particle with coordinates (v_x, v_y, v_z) in an effective potential

$$U(v_x, v_y, v_z) = \frac{1}{2} (\lambda_x^2 v_x^2 + \lambda_y^2 v_y^2 + \lambda_z^2 v_z^2) + \frac{1}{2} \left(\frac{1}{v_x^2} + \frac{1}{v_y^2} + \frac{1}{v_z^2} \right)$$

$$+ \frac{P}{v_x v_y v_z} \left[1 + \frac{u_2}{g} \int d\mathbf{r} \right.$$

$$\left. \times \exp\left(-\sum_\eta \frac{\eta^2}{2v_\eta^2} \right) \frac{Y_{20}(\theta)}{r^3} \right]. \quad (8)$$
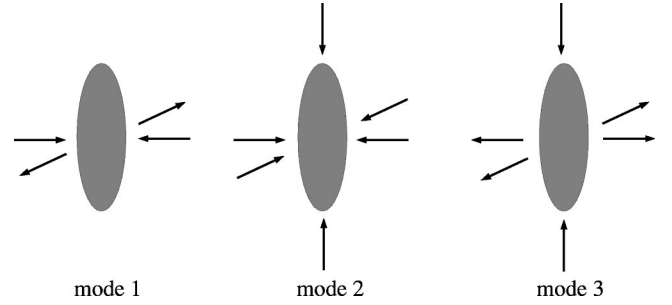

FIG. 1. Graphical representation of oscillations modes of the condensate.

Small amplitude oscillations around the stationary solution can be found by studying second derivatives of U. This procedure provides the excitation frequency for the first three compressional excitation modes of the system [11]. The geometry of these modes is depicted in Fig. 1. For cylindrical traps with the axis along the dipole direction, the projection of the angular momentum, m, on the z axis is a good quantum number. For modes 2 and 3 we have $m=0$, whereas $m=1$ for mode 1. In the following we call mode 2 (3) the breathing (quadrupole) mode.

B. The nature of the instability

To study the nature of the instability, one needs to determine which mode becomes unstable when the number of atoms reaches the critical value and to describe the behavior of the frequency of the corresponding mode close to the criticality. These two issues have been first discussed for the case of short-range interacting Bose gases with $a<0$. Bergeman [32] observed numerically that, as the ratio γ of the nonlinear interaction energy to the trap frequency approaches a given critical value γ_c, the frequency of the breathing mode tends to zero and merges with the frequency of the Goldstone mode corresponding to the overall phase of the condensate. Above the criticality, the breathing mode becomes unstable and attains complex frequency. Singh and Rokhsar [30] analyzed this instability using self-similar solutions describing the modes (equivalently one may employ the variational approach of the preceding section). They have shown that close to the criticality the frequency of the breathing mode 2 vanishes as $|\gamma - \gamma_c|^{1/4}$.

In the case of a dipolar gas with dominant dipole interactions the situation is completely different and much more complex. Only for aspect ratios far above the criticality, $l \gg l^*$ ($l > 1.29$), the situation resembles that of a gas with $a < 0$. The mode corresponding to the lowest frequency is the breathing mode. This mode becomes unstable when the parameter $\sigma \to \sigma_c$. The scaling behavior of the frequency of this mode can be analyzed employing the variational approach of the preceding section [11]. We find that ω_2 goes to zero as $(\sigma_c - \sigma)^\beta$, with $\beta \approx 1/4$. For intermediate values of $l > l^*$ ($0.75 < l < 1.29$) the exponent β is still $1/4$, but the geometry of the mode which drives the instability depends on σ. For σ far below σ_c the mode corresponding to the lowest frequency has a breathing symmetry, whereas as one approaches the critical value of σ the lowest mode becomes

quadrupolelike. For l close to l^* ($l<0.75$) the situation changes and the mode corresponding to the lowest frequency is quadrupolarlike. For l not too close to l^* the exponent β is still close to 1/4. However, as l approaches l^*, the exponent β departs from 1/4 towards a greater value, which becomes 2 at $l=l^*$. The latter prediction must be understood as a qualitative argument, since for l very close to l^*, the system enters a Thomas-Fermi regime where the Gaussian ansatz is no more valid.

C. Numerical results

In this section we study the low-lying collective excitations of a trapped dipolar BEC by analyzing numerically the response of a BEC after applying an external perturbation. We compare our numerical results with those obtained from the variational approach described above. In the following, we employ the method introduced in Ref. [42] for the case of a short-range interacting BEC. After generating the BEC ground-state wave function using imaginary time evolution of the GPE, we first slightly perturb the trapping potential in a periodic way:

$$V(\mathbf{r},t)=\frac{1}{2}m\sum_{\eta=x,y,z}[1+A_\eta\sin(\omega_{mod}t+\alpha_\eta)]^2\omega_\eta^2\eta^2,$$

$$(9)$$

where ω_{mod} is the modulation frequency, A_η are the amplitudes, and α_η are the initial phases. A perturbation of a chosen symmetry can be accomplished by properly selecting these parameters. In particular, sufficiently small amplitudes are necessary near the instabilities, since the system can be easily driven into collapse. On the other hand, by setting large amplitudes one may probe various nonlinear effects [42,43]. The response of the system is enhanced by selecting ω_{mod} in the vicinity of expected excitation frequencies.

In a second stage, the condensate evolves in an unperturbed trap (i.e., $A_\eta=0$). The condensate widths are monitored and subsequently Fourier transformed to reveal the excitation spectrum. Our aim is to determine the (potentially small) deviations of the excitation frequencies with respect to those expected for purely short-range interacting gases, as precisely as they can be experimentally measured (typically $\Delta\omega/\omega_{trap}\simeq0.01$ [28,29]). Long integration times are necessary to accomplish the desired spectral resolution. This introduces serious technical difficulties, since a large number of integration steps is needed to guarantee the energy conservation during the whole evolution. Note that additional complications arise from the evaluation of the interaction integral in Eq. (1) at each time step.

1. Dominant dipole-dipole interactions

For the case of dominant dipole-dipole interactions [10], the short-range part of Eq. (1) can be safely omitted. We consider two different trap geometries that were employed at JILA in Ref. [28], with a trap aspect ratio $l=8^{-1/4}$ (referred to as pancake JILA trap), and a trap with $l=8^{1/4}$ (referred to as cigar JILA trap). The latter trap has been recently employed for experiments in ^{85}Rb [26].
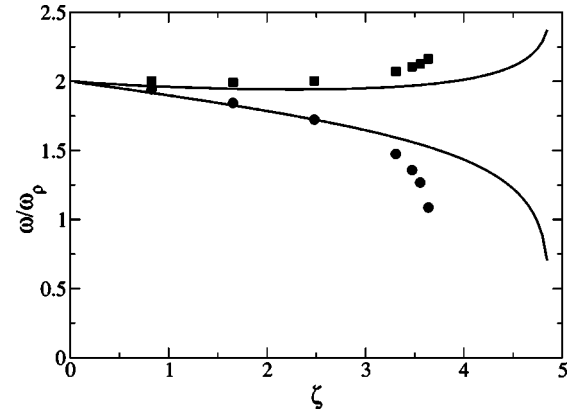

FIG. 2. Numerical results for the excitation frequencies of modes 1 (squares) and 3 (circles) as functions of the dipolar parameter ζ for a gas of condensed dipoles in the pancake JILA trap. The solid lines indicate the corresponding variational results.

In the following, we study the excitation frequencies as a function of the dipolar parameter

$$\zeta=N\frac{m}{\hbar^2}\sqrt{\frac{m\omega_\rho}{\hbar}}d^2. \tag{10}$$

Note the relation $\sigma=2\sqrt{2\omega_\rho/\omega_{min}}\zeta$. Since in the pancake JILA trap the breathing mode has a relatively high frequency and it is not excited by the perturbation of the GPE, we concentrate in this case on the modes 1 and 3 of Fig. 1. The results for the pancake JILA trap are presented in Fig. 2. For $\zeta=0$ the ideal-gas result $\omega/\omega_\rho=2$ is retrieved for both modes 1 and 3. As ζ increases mode 1 is shifted upwards, whereas the frequency of mode 3 (quadrupole) goes down, vanishing for a critical ζ_{cr} at which the system becomes unstable. Probing the system in this regime is very difficult, since even a slight disturbance drives the collapse. For $\zeta>\zeta_{cr}\approx3.68$, it is not possible to obtain stable ground-state solutions of the time-independent GPE [10]. The variational analysis reproduces the numerical results for relatively weak dipolar interactions. However, it does not describe well the numerical results close to the instability.

Figure 3 depicts a similar dependence for the cigar JILA trap. In this case the breathing mode is the lowest one. The frequency of mode 1 displays an upward shift whereas that of the quadrupole mode stays essentially untouched. Again, the instability threshold is not correctly predicted by the variational analysis.

2. Interplay between short-range and dipole-dipole interactions

Let us now consider the case in which the short-range interactions and the dipole-dipole ones have a comparable strength [8,9,13,12,11]. In particular, we have performed our simulations for the particular case of ^{52}Cr, which has drawn some experimental interest [19–23], since it possesses a large magnetic dipole moment of $6\mu_B$ (Bohr magnetons). The value of a for this element is at the moment unknown, and consequently we have explored different values of a in the calculations below. In the following, the trap parameters
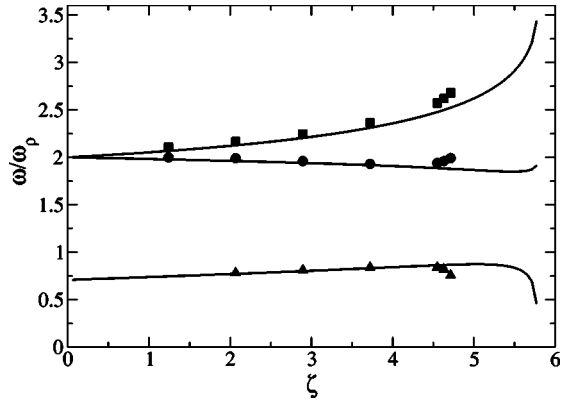
FIG. 3. Numerical results for the excitation frequencies of modes 1 (squares), 2 (triangles), and 3 (circles) as functions of the dipolar parameter ζ for a gas of condensed dipoles in the cigar JILA trap. The solid lines indicate the corresponding variational results.

correspond to those of an ongoing experiment in Stuttgart [40], namely, $\omega_z = 2\pi \times 40$ Hz and $\omega_\rho = 2\pi \times 485$ Hz.

Figure 4 shows the three lowest modes for different values of a, for the case of $N = 10\,000$ atoms. When a is smaller than a_{crit}, the system becomes unstable due to an unbalanced attractive component of dipole-dipole interactions [8,9,13,11]. When approaching $a^{crit}/a_{Na} \simeq 0.23$ from above, the frequency of the lowest mode decreases to 0 and the system collapses. For $0.23 < a/a_{Na} < 0.26 a_{Na}$ the lowest mode (triangles) has a breathing geometry, whereas the highest one (circles) is quadrupolelike. The opposite is true for $a/a_{Na} > 0.26 a_{Na}$. The highest mode shows virtually no dependence on the scattering length whereas the frequency of mode 1 is shifted upwards. Again, close to the instability, the results obtained from the variational calculation differ from those obtained numerically. Moreover, the behavior of the
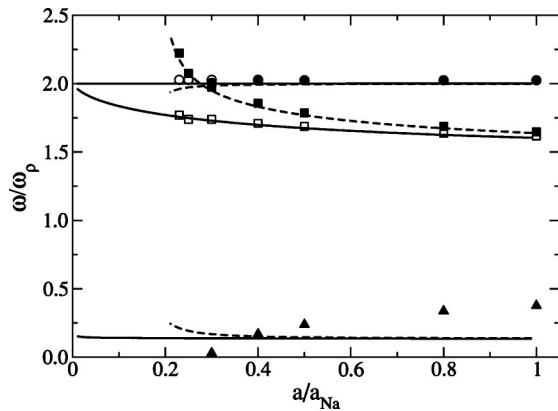

FIG. 4. Excitation frequencies of modes 1 (filled squares), highest (filled triangles) and lowest (filled circles) as functions of the scattering length (expressed in units of the corresponding value for sodium) for a condensate of 10 000 chromium atoms in a trap with $\omega_z = 2\pi \times 40$ Hz and $\omega_\rho = 2\pi \times 485$ Hz (numerical results). The corresponding variational values are depicted by dashed lines. Solid lines indicate variational data for the case with no dipole-dipole interactions and the corresponding numerical results are plotted with empty symbols (note that we have not been able to probe the lowest mode numerically).
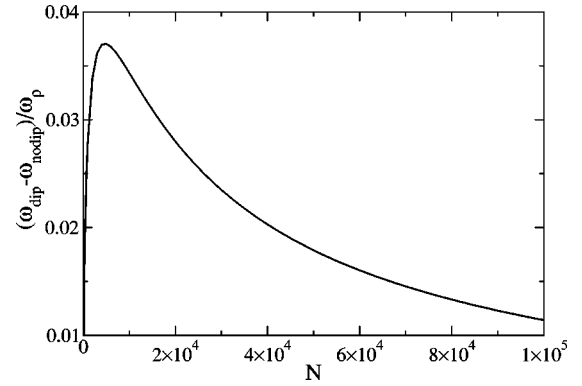

FIG. 5. Difference of excitation frequency for mode 1 in the absence and in the presence of dipole-dipole interactions, as a function of the total number of atoms N, for $a = a_{Na}$ and a trap aspect ratio $l = \sqrt{485/40}$ (data from the variational analysis).

lowest mode is not reproduced correctly even qualitatively. Figure 4 also presents the excitation frequencies for the same system in the absence of dipole-dipole interactions. Apart from the obvious presence of the instability in the dipolar case (and the corresponding behavior of the lowest mode) we observe large frequency differences for mode 1 between the cases with and without dipole-dipole interactions.

The above result suggests that the effects of dipole-dipole interactions may be detectable. Having discussed the role of a, it is thus important to discuss the possible values of N and ω_ρ / ω_z, which could maximize the dipole-induced frequency shifts.

Figure 5 shows the deviation between the case with and without dipole-dipole interactions, for the mode 1, $\omega_z / \omega_\rho = 40/485$, and $a = a_{Na}$. For this calculation we have employed the variational method as it is very exact away from the instability. We observe that for number of atoms N greater than 5000 the frequency shift is observable (i.e., greater than 0.01), and reaches its maximum ($\gtrsim 3.5\%$) for $N \simeq 10\,000$ which should be the number available in ongoing experiments [40]. In this case, shifts for modes 2 and 3 are substantially lower ($\simeq 0.001$).

Finally, we have analyzed (using the variational method) the dependence of the spectrum on the trap aspect ratio l for $a = a_{Na}$ and $N = 10\,000$. The results are presented in Fig. 6. We observe that in pancake traps with $l < 0.7$, the quadrupole mode experiences a shift of up to 10% with respect to the nondipolar case. We have confirmed this conclusion by performing an exact numerical simulation of the perturbed GPE for $l = 0.58$, $a = a_{Na}$, and $N = 10\,000$. For these parameters the excitation frequency of mode 3 is $1.76\omega_\rho$ ($1.86\omega_\rho$) with (without) dipole-dipole interactions. The remaining two modes also display large shifts over a wide range of aspect ratios.

IV. BALLISTIC EXPANSION OF A DIPOLAR BEC

In typical BEC experiments, the measurements are performed after removing the trapping potential and allowing for a ballistic expansion of the condensate. It is the aim of
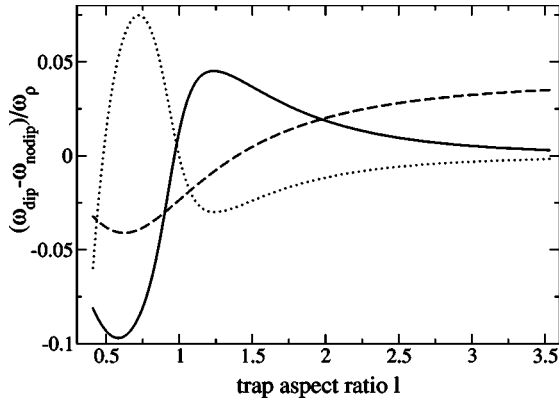
FIG. 6. Difference of excitation frequency for modes 1 (dashed line), breathing (dotted line), and quadrupolelike (solid line) between the cases of purely contact and mixed (contact and dipole-dipole) interactions as a function of the trap aspect ratio for 10 000 atoms and $a = a_{Na}$ (data from variational analysis).

this section to briefly discuss such an expansion by means of the previously introduced variational approach. After evaluating the minimum of the potential provided by Eq. (8), i.e., the ground state of the trapped gas, we set $\lambda_{x,y,z} = 0$ in Eq. (7) and evolve these equations using the ground state as an initial condition. In this section we restrict ourselves to the case of dominant dipole-dipole interactions.

The ballistic expansion of a short-range interacting BEC is characterized by an inversion of the aspect ratio of the condensate cloud, i.e., cigar-shaped condensates become pancakelike after expansion, and vice versa. This is not necessarily the case in dipolar condensates. Figure 7 shows the condensate aspect ratio for a spherical trap, before releasing the trap (dashed), and once the aspect ratio reaches a stationary value after the expansion (solid). The aspect ratio of the cloud decreases during the expansion, but never becomes smaller than 1, i.e., the condensate keeps its original cigar-shaped character during the expansion. A similar behavior is observed for $1 < l < 1.12$, where there exists a range of ζ values for which the BEC remains cigarlike. For $l^* < l < 1$ and for ζ close to ζ_{cr}, the BEC also remains cigar shaped
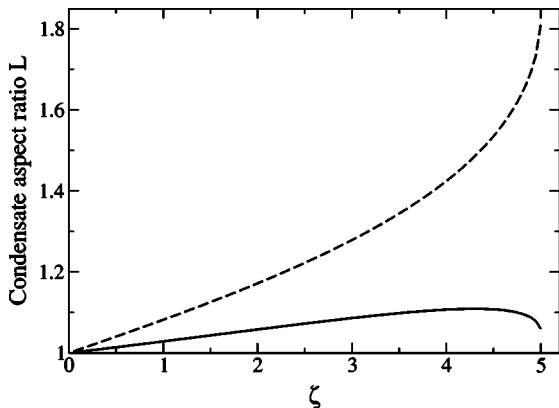

FIG. 7. Aspect ratio as a function of σ for a condensate initially trapped in a spherical trap of frequency ω, before the expansion (dashed) and after $48.5\omega^{-1}$ (solid).

during the time of flight. On the contrary, for $l > 1.12$ the cloud becomes pancakelike after expanding for all ζ; and for $l < l^*$, the initial pancake cloud always becomes cigar shaped.

V. GROUND STATE OF A BINARY DIPOLAR BEC

In the previous sections we have shown that various phenomena are expected in dipolar BEC. One can therefore expect that even a richer behavior can be displayed by a multicomponent dipolar BEC. In the case of two-component dipolar gases, the system properties depend on a large number of control parameters, including the number of particles in each component, the strengths and orientations of the dipoles, and the trap geometries. In the following, for simplicity, we focus on the case of a BEC of two dipolar identical components polarized in opposite directions. As discussed in Sec. I this should be the case for Hund A molecules in a magnetic field, where the magnetic moment is oriented by the field, but the (possibly large) electric moment can be parallel or antiparallel to the direction of the applied magnetic field. To simplify the analysis even further, we consider only a spherical trap. Thus, the system is determined by ζ and $\eta = N_1/N$, where as before N is the total number of particles and N_1 is the number of particles in the component 1. The system can be described by a system of two coupled GPEs:

$$i\dot{\psi}_1 = \left\{ -\frac{\nabla^2}{2} + \frac{r^2}{2} + + \zeta[\, \eta V_1(\mathbf{r}) - (1-\eta)V_2(\mathbf{r})] \right\} \psi_1,$$
(11a)

$$i\dot{\psi}_2 = \left\{ -\frac{\nabla^2}{2} + \frac{r^2}{2} + + \zeta[\, -\eta V_1(\mathbf{r}) + (1-\eta)V_2(\mathbf{r})] \right\} \psi_2,$$
(11b)

where $V_i(\mathbf{r}) = \int d\mathbf{r}'(1 - 3\cos^2\theta)|\psi_i(\mathbf{r}',t)|^2/|\mathbf{r} - \mathbf{r}'|^3$. In the above expression we have employed harmonic oscillator units of length $\sqrt{\hbar/m\omega}$. For equal population of the components ($\eta = 0.5$) both ground-state wave functions are the same. As a consequence, the nonlocal interaction terms vanish and the system behaves like an ideal gas, the ground-state wave functions being that of the corresponding harmonic oscillator. However, as the interaction strength ζ increases, the system becomes unstable. The reason of this instability is rooted in the excitation spectrum and is discussed below.

For each value of η it is possible to compute a critical ζ_{cr} above which no stable solution of Eqs. (11) exists. The corresponding stability diagram, resulting from a numerical solution of Eqs. (11), is presented in Fig. 8. We observe that the more symmetric the mixture is, the more stable it is.

For $\eta \neq 0.5$ the ground state has a more complicated structure. In this respect it resembles solutions for short-range interacting binary condensates [35,36]. In particular, the component whose self-interaction is stronger partially wraps around the other. However, contrary to short-range interacting binary BEC, due to the anisotropy of the dipole-dipole interactions, the density dip in one component appears only
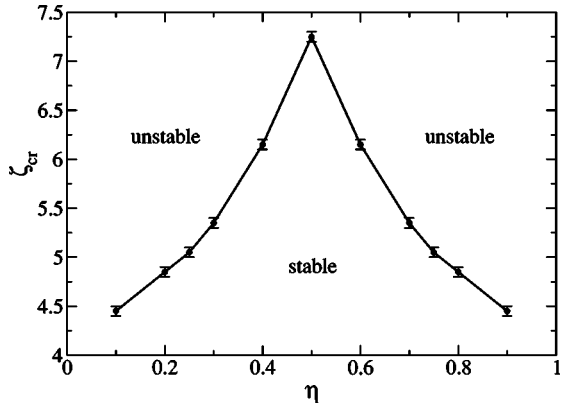
FIG. 8. Stability diagram for a binary condensate of oppositely polarized dipolar gases in a spherically symmetric trap. Above the line there are no stable ground-state solutions.

along the radial direction, whereas along z both components possess Gaussian profiles. An example of such a structure is shown in Fig. 9.

In the analysis presented in this section we have neglected the influence of short-range interactions. Since the two components are identical except for the opposite dipole moments, the short-range interactions (both intercomponent and the intracomponent ones) are the same. Therefore, in the absence of dipole-dipole interactions a miscible mixture is expected, which differs from the ideal-gas Gaussian case considered above (eventually acquiring a Thomas-Fermi profile). However, in the same way as above, the dipole-dipole mean fields will be exactly canceled for $\eta = 0.5$. Therefore, the cloud is expected to remain in an unperturbed Thomas-Fermi profile until the ζ coefficient reaches a critical value ζ_{cr} (only quantitatively different from that obtained in absence of short-range interactions). For $\zeta > \zeta_{cr}$ the system becomes unstable.

VI. EXCITATIONS OF A BINARY DIPOLAR BEC

In this section we analyze the excitation spectrum of the previously discussed gas of two oppositely oriented dipolar
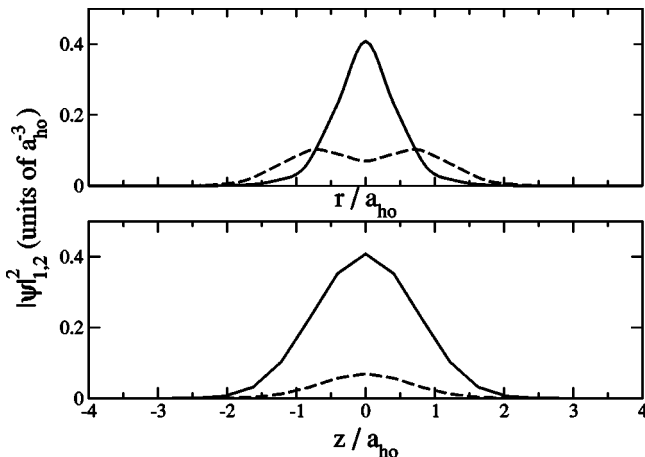

FIG. 9. Density profiles along the radial (upper graph) and axial (lower graph) directions for a binary condensate of two oppositely polarized dipolar gases. Parameters are $\eta = 0.8$ and $\zeta = 4.8$.

components. We first discuss the homogeneous case, and then study the case of harmonically trapped binary dipolar BEC.

A. Homogeneous space

Let us consider two species of dipoles $\mathbf{d}_1 = d_1 \mathbf{u}_z$ and $\mathbf{d}_2 = -d_2 \mathbf{u}_z$ with respective densities n_1 and n_2 in a homogeneous box of volume V. The Hamiltonian in second quantization is

$$\hat{H} = \sum_{\mathbf{k}\alpha=1,2} \frac{\hbar^2 \mathbf{k}^2}{2m} a_{\mathbf{k}\alpha}^\dagger a_{\mathbf{k}\alpha}$$
$$+ \frac{1}{2} \sum_{\alpha=1,2} \sum_{\mathbf{k}_1,\mathbf{k}_2,\mathbf{k}_1',\mathbf{k}_2'} g(\mathbf{k}_1',\mathbf{k}_2';\mathbf{k}_1,\mathbf{k}_2) a_{\mathbf{k}_1'\alpha}^\dagger a_{\mathbf{k}_2'\alpha}^\dagger a_{\mathbf{k}_2\alpha} a_{\mathbf{k}_1\alpha}$$
$$- \sum_{\mathbf{k}_1,\mathbf{k}_2,\mathbf{k}_1',\mathbf{k}_2'} g(\mathbf{k}_1',\mathbf{k}_2';\mathbf{k}_1,\mathbf{k}_2) a_{\mathbf{k}_1'1}^\dagger a_{\mathbf{k}_2'2}^\dagger a_{\mathbf{k}_2 2} a_{\mathbf{k}_1 1}, \quad (12)$$

with

$$g(\mathbf{k}_1',\mathbf{k}_2';\mathbf{k}_1,\mathbf{k}_2) = \int d\mathbf{r} \int d\mathbf{r}' \psi_{\mathbf{k}_1'}^*(\mathbf{r}) \psi_{\mathbf{k}_2'}^*(\mathbf{r}') V(\mathbf{r}-\mathbf{r}')$$
$$\times \psi_{\mathbf{k}_2}(\mathbf{r}') \psi_{\mathbf{k}_1}(\mathbf{r}), \quad (13)$$

and $a_{\mathbf{k}i}$ the annihilation operator of a particle of the ith component with momentum $\mathbf{k}$. Performing the Bogoliubov approximation ($a_{01}^\dagger = a_{01} = \sqrt{N_1}$ and $a_{02}^\dagger = a_{02} = \sqrt{N_2}$), one obtains

$$\hat{H} = \sum_{\mathbf{k}\neq 0} \{ [\epsilon_\mathbf{k} + 2B(\hat{\mathbf{k}})] a_{\mathbf{k}1}^\dagger a_{\mathbf{k}1} + [\epsilon_\mathbf{k} + 2\lambda^2 B(\hat{\mathbf{k}})] a_{\mathbf{k}2}^\dagger a_{\mathbf{k}2}$$
$$+ B(\hat{\mathbf{k}}) [(a_{\mathbf{k}1}^\dagger a_{-\mathbf{k}1}^\dagger + a_{\mathbf{k}1} a_{-\mathbf{k}1}) + \lambda^2 (a_{\mathbf{k}2}^\dagger a_{-\mathbf{k}2}^\dagger + a_{\mathbf{k}2} a_{-\mathbf{k}2})$$
$$- 2\lambda (a_{\mathbf{k}1} a_{-\mathbf{k}2} + a_{\mathbf{k}1}^\dagger a_{-\mathbf{k}2} + a_{\mathbf{k}1}^\dagger a_{\mathbf{k}2} + a_{\mathbf{k}2}^\dagger a_{\mathbf{k}1})] \}, \quad (14)$$

with $\epsilon_\mathbf{k} = \hbar^2 \mathbf{k}^2/2m$, $\sqrt{n_2 d_2^2} = \lambda \sqrt{n_1 d_1^2}$, and $B(\hat{\mathbf{k}}) = (8\pi/3)\sqrt{(\pi/5)}(n_1 d_1^2) Y_{20}(\hat{\mathbf{k}})$. The diagonalization of the Hamiltonian provides two different branches of quasiparticle excitations:

$$E_1 = \epsilon_\mathbf{k}, \quad (15a)$$

$$E_2 = \left(\epsilon_\mathbf{k}^2 + \frac{32\pi}{3} \sqrt{\frac{\pi}{5}} (1+\lambda^2)(n_1 d_1^2) Y_{20}(\hat{\mathbf{k}}) \epsilon_\mathbf{k} \right)^{1/2}. \quad (15b)$$

For the case of $\lambda \to 0$, the spectrum of a homogeneous single-component dipolar BEC is discussed in Sec. II. As observed, the spectra (15a) is that of a soft mode, whereas the second branch (15b) is even more unstable than that of a single-component BEC.

B. Trapped case

For simplicity, we limit ourselves to the case of a spherical trap with frequency ω, but similar arguments can be em-

ployed for a cylindrical trap. We also consider $|\mathbf{d}_1|=|\mathbf{d}_2|$ and $\eta=0.5$ (i.e., $N_1=N_2=N/2$). As we have already noted, in this case the ground state of the system is the ground state of a harmonic oscillator. It is therefore more convenient to rewrite the Hamiltonian in terms of the creation and annihilation operators of the harmonic oscillator modes for the dipole components 1 and 2:

$$\hat{H}=\sum_{\mathbf{n}} \hbar\omega_{\mathbf{n}}(a^{\dagger}_{\mathbf{n}1}a_{\mathbf{n}1}+a^{\dagger}_{\mathbf{n}2}a_{\mathbf{n}2})$$

$$+\frac{N_1 d^2}{2}\sum_{\mathbf{n}_1,\mathbf{n}_2\neq 0}\{g(\mathbf{n}_1,\mathbf{n}_2;0,0)a^{\dagger}_{\mathbf{n}_1 1}a^{\dagger}_{\mathbf{n}_2 1}$$

$$+g(0,0;\mathbf{n}_1,\mathbf{n}_2)a_{\mathbf{n}_1 1}a_{\mathbf{n}_2 1}+g(\mathbf{n}_1,\mathbf{n}_2;0,0)a^{\dagger}_{\mathbf{n}_1 2}a^{\dagger}_{\mathbf{n}_2 2}$$

$$+g(0,0;\mathbf{n}_1,\mathbf{n}_2)a_{\mathbf{n}_1 2}a_{\mathbf{n}_2 2}+2g(\mathbf{n}_1,0;\mathbf{n}_2,0)a^{\dagger}_{\mathbf{n}_1 1}a_{\mathbf{n}_2 1}$$

$$+2g(\mathbf{n}_1,0;\mathbf{n}_2,0)a^{\dagger}_{\mathbf{n}_1 2}a_{\mathbf{n}_2 2}$$

$$-2g(0,0;\mathbf{n}_1,\mathbf{n}_2)a_{\mathbf{n}_1 1}a_{\mathbf{n}_2 2}$$

$$-2g(\mathbf{n}_1,\mathbf{n}_2;0,0)a^{\dagger}_{\mathbf{n}_1 1}a^{\dagger}_{\mathbf{n}_2 2}-2g(\mathbf{n}_1,0;0,\mathbf{n}_2)a^{\dagger}_{\mathbf{n}_1 1}a_{\mathbf{n}_2 2}$$

$$-2g(\mathbf{n}_1,0;0,\mathbf{n}_2)a^{\dagger}_{\mathbf{n}_1 2}a_{\mathbf{n}_2 1}\}, \tag{16}$$

where $\mathbf{n}\equiv(n,l,m)$ denotes the set of spherical quantum numbers for the corresponding eigenstate of the harmonic oscillator, $\hbar\omega_{\mathbf{n}}$ is the energy of the eigenstate $\mathbf{n}$, and

$$g(\mathbf{n}_1,\mathbf{n}_2;\mathbf{n}_3,\mathbf{n}_4)=\int dr\int dr'\,\psi^{*}_{\mathbf{n}_1}(r)\psi^{*}_{\mathbf{n}_2}(r')V(r-r')$$

$$\times\psi_{\mathbf{n}_3}(r')\psi_{\mathbf{n}_4}(r). \tag{17}$$

Let us perform the Bogoliubov transformation

$$b_{\nu}=\sum_{\mathbf{n}\neq 0}(u_{\nu\mathbf{n}}a_{\mathbf{n}1}+v_{\mathbf{n}\nu}a^{\dagger}_{\mathbf{n}1}+\tilde{u}_{\nu\mathbf{n}}a_{\mathbf{n}2}+\tilde{v}_{\mathbf{n}\nu}a^{\dagger}_{\mathbf{n}2}), \tag{18}$$

which satisfies $\epsilon_{\nu}b_{\nu}=[b_{\nu},\hat{H}]$, leading to the corresponding Bogoliubov-de Gennes (BdG) equations. Such equations can be simplified by taking the more appropriate variables $A_{\nu\mathbf{n}}=u_{\nu\mathbf{n}}+\tilde{u}_{\nu\mathbf{n}}$, $B_{\nu\mathbf{n}}=v_{\nu\mathbf{n}}+\tilde{v}_{\nu\mathbf{n}}$, $C_{\nu\mathbf{n}}=u_{\nu\mathbf{n}}-\tilde{u}_{\nu\mathbf{n}}$, $D_{\nu\mathbf{n}}=v_{\nu\mathbf{n}}-\tilde{v}_{\nu\mathbf{n}}$. Then, the BdG equations take the form:

$$\epsilon_{\nu}A_{\nu\mathbf{n}}=\hbar\omega_{\mathbf{n}}A_{\nu\mathbf{n}}, \tag{19a}$$

$$\epsilon_{\nu}B_{\nu\mathbf{n}}=-\hbar\omega_{\mathbf{n}}B_{\nu\mathbf{n}}, \tag{19b}$$

$$\epsilon_{\nu}C_{\nu\mathbf{n}}=\hbar\omega_{\mathbf{n}}C_{\nu\mathbf{n}}+2N_1 d^2\sum_{\mathbf{n}'\neq 0}\{g(\mathbf{n}',0;\mathbf{n},0)C_{\nu\mathbf{n}'}$$

$$-g(0,0;\mathbf{n},\mathbf{n}')D_{\nu\mathbf{n}'}\}, \tag{19c}$$

$$\epsilon_{\nu}D_{\nu\mathbf{n}}=-\hbar\omega_{\mathbf{n}}D_{\nu\mathbf{n}}+2N_1 d^2\sum_{\mathbf{n}'\neq 0}\{g(\mathbf{n},\mathbf{n}';0,0)C_{\nu\mathbf{n}}$$

$$-g(\mathbf{n},0;\mathbf{n}',0)D_{\nu\mathbf{n}'}\}. \tag{19d}$$

In the following, we omit, for simplicity, ν in the notation for the A, B, C, and D coefficients. We observe that, like in the homogeneous case, we have two different branches of quasiparticles, one of them being a soft mode. The last two equations are the BdG equations for the nonsoft mode. From the properties of spherical harmonics and the $3j$ symbols, it is possible to obtain that

$$g(0,0;nlm,n'l'm')=g(nlm,n'l'm';0,0)$$

$$=g(0,0;nlm,n'l'-m)\delta_{m',-m}$$

$$\times g(nlm,0;n'l'm',0)$$

$$=g(n'l'm',0;nlm,0)$$

$$=g(0,0;nlm,n'l'-m)\delta_{m',m}.$$

Also, $l'=l,l\pm 2$ must be fulfilled. Employing these properties, and changing to the variables $F_{nlm}=C_{nlm}-(-1)^m D_{nl-m}$, $G_{nlm}=C_{nlm}+(-1)^m D_{nl-m}$, one obtains that $G_{nlm}=(\epsilon/\hbar\omega_n)F_{nlm}$, and

$$\epsilon^2 F_{nlm}=(\hbar\omega_n)^2 F_{nlm}+4N_1 d^2\hbar\omega_n$$

$$\times\sum_{n\neq 0}g(0,0;nlm,n'l'-m)F_{n'l'm}. \tag{20}$$

One can write

$$g(0,0;nlm,n'l'm')=(-1)^{(l'-l)/2}\frac{1}{2\sqrt{2}a_0^3}h(n,l;n',l')$$

$$\times\langle l'm|l,m|20\rangle, \tag{21}$$

where $a_0=\sqrt{\hbar/2m\omega}$. In Eq. (21) the angular contribution is given by

$$\langle l',m|lm|20\rangle=(-1)^m\begin{pmatrix}l'l2\\-mm0\end{pmatrix}\begin{pmatrix}l'l2\\000\end{pmatrix}$$

$$\times\left[\frac{5(2l+1)(2l'+1)}{4\pi}\right]^{1/2}, \tag{22}$$

whereas the coefficients $h(n,l;n',l')$ constitute the radial contribution and are of the form

$$h(n,l;n',l') = \frac{8}{3\sqrt{5}} \frac{1}{2^{(n+n')/2}} \frac{\Gamma\left(\frac{n+n'+3}{2}\right)}{\sqrt{\Gamma\left(\frac{n+l+3}{2}\right)\Gamma\left(\frac{n-l+2}{2}\right)\Gamma\left(\frac{n'+l'+3}{2}\right)\Gamma\left(\frac{n'-l'+2}{2}\right)}}. \quad (23)$$

Then the problem reduces to finding the eigenvalues of the following equation:

$$\epsilon^2 F_{nlm} = n^2 F_{nlm} + \sqrt{2}\zeta n \sum_{l'=l,l\pm2} \sum_{n'\geqslant l'} (-1)^{(l-l')/2} h$$

$$\times (nl;n'l')\langle l'm|lm|20\rangle F_{n'l'm}, \quad (24)$$

where ζ is defined in Eq. (10), and ϵ is in units of $(\hbar\omega)^2$. From the analysis of the spectrum one can observe that for $\zeta > \zeta_{cr} = 6.7$ the energy of the lowest state of the subspace $n=2$, $m=0$ becomes imaginary. Therefore, although the ground state of the mixture of antiparallel dipolar components is that of an ideal gas, the system will eventually become unstable for $\eta > \eta_{cr}$ due to the appearance of imaginary excitation frequencies. The value of ζ_{cr} compares very well with the numerically found value of $\zeta_{cr} \simeq 7.3$ for the onset of the instability.

Finally, it is interesting to analyze the situation in which $\zeta \ll 1$, since in this situation the states with different n do not mix, and one can analytically diagonalize in each n subspace. The first excited states are [in units of $(\hbar\omega)^2$]

$$\epsilon^2(n=1,l=1,m=0) = 1 + 4\sqrt{2/\pi}\zeta/15, \quad (25)$$

$$\epsilon^2(n=1,l=1,m=\pm1) = 1 - 2\sqrt{2/\pi}\zeta/15, \quad (26)$$

$$\epsilon^2(n=2,l=\{2,0\},m=0) = 4 + (2\pm\sqrt{102})\sqrt{2/\pi}\zeta/21, \quad (27)$$

$$\epsilon^2(n=2,l=2,m=\pm1) = 4 + 2\sqrt{2/\pi}\zeta/21. \quad (28)$$

From these expressions it becomes clear that, for example, in the subspace of states with $n=2$, $m=0$ (which is an admixture of the noninteracting quadrupole and monopole modes) even for $\zeta \sim 0.1$ deviations of more than 1% are expected. One can also observe that vortices with vorticity in the dipole direction are less energetic than those with vorticity in the plane perpendicular to the dipole direction.

VII. CONCLUSIONS

In this paper we have analyzed the ground state and the excitation spectrum of single- and two-component dipolar condensates. For the case of single-component BECs we have shown that their stability properties are determined by the trapping geometry. In particular, for sufficiently pancake-like traps the condensate is always stable and independent of the number of particles. We have then analyzed the excitation spectrum of the single-component condensate by analyzing the response of the condensate to small perturbations and comparing the results with analytical calculations based on a variational approach. We have discussed in detail the nature of the instability and associated it with vanishing of frequency of one of the excitation modes. The scaling behavior of this frequency was also analyzed. We have discussed different possible scenarios in which the dipole-dipole effects could have observable effects even in the presence of a dominant short-range interaction. This analysis could be of special interest for ongoing experiments on atoms with large magnetic moments, such as chromium [39]. We have provided guidelines for experimental parameters corresponding to largest discrepancies between the cases with and without dipole-dipole interactions. In the second part of the paper we have analyzed the properties of a two-component BEC of dipolar particles. In particular, we have studied the stability of the ground state as a function of the relative density of both species as well as the appearance of phase separation in the binary condensate. Finally, we have obtained the excitation spectrum for this particular physical system and discussed the nature of its instability.

[1] M.H. Anderson, J.R. Ensher, M.R. Matthews, C.E. Wieman, and E.A. Cornell, Science **269**, 198 (1995); K.B. Davis, M.-O. Mewes, M.R. Andrews, N.J. van Druten, D.S. Durfee, D.M. Kurn, and W. Ketterle, Phys. Rev. Lett. **75**, 3969 (1995); D.G. Fried, T.C. Killian, L. Willmann, D. Landhuis, S.C. Moss, D. Kleppner, and T.J. Greytak, *ibid.* **81**, 3811 (1998); S.L. Cornish, N.R. Claussen, J.L. Roberts, E.A. Cornell, and C.E. Wieman, *ibid.* **85**, 1795 (2000); A. Robert, O. Sirjean, A. Browaeys, J. Poupard, S. Nowak, D. Boiron, C.I. Westbrook, and A. Aspect, Science **292**, 461 (2001); F. Pereira Dos Santos, J. Leonard, J. Wang, C.J. Barrelet, F. Perales, E. Rasel, C.S. Unnikrishnan, M. Leduc, and C. Cohen-Tannoudji, Phys. Rev. Lett. **86**, 3459 (2001); G. Modugno, G. Ferrari, G. Roati, R.J. Brecha, A. Simoni, and M. Inguscio, Science **294**, 1320 (2001).

[2] C.C. Bradley, C.A. Sackett, J.J. Tollett, and R.G. Hulet, Phys. Rev. Lett. **75**, 1687 (1995); **79**, 1170(E) (1997).

[3] See, for example, F. Dalfovo, S. Giorgini, L.P. Pitaevskii, and S. Stringari, Rev. Mod. Phys. **71**, 463 (1999).

[4] J.M. Gerton, D. Strekalov, I. Prodan, and R.G. Hulet, Nature (London) **408**, 692 (2000).

[5] P.A. Ruprecht, M.J. Holland, K. Burnett, and M. Edwards, Phys. Rev. A **51**, 4704 (1995).

[6] G. Baym and C.J. Pethick, Phys. Rev. Lett. **76**, 6 (1996).

[7] Y. Kagan, G.V. Shlyapnikov, and J.T.M. Walraven, Phys. Rev. Lett. **76**, 2670 (1996).

[8] S. Yi and L. You, Phys. Rev. A **61**, 041604 (2000).

[9] K. Góral, K. Rzążewski, and T. Pfau, Phys. Rev. A **61**, 051601 (2000).

[10] L. Santos, G.V. Shlyapnikov, P. Zoller, and M. Lewenstein, Phys. Rev. Lett. **85**, 1791 (2000).

[11] S. Yi and L. You, Phys. Rev. A **63**, 053607 (2001).

[12] S. Yi and L. You, Phys. Rev. A **66**, 013607 (2002).

[13] J.-P. Martikainen, M. Mackie, and K.-A. Suominen, Phys. Rev. A **64**, 037601 (2001).

[14] H. Pu, W. Zhang, and P. Meystre, Phys. Rev. Lett. **87**, 140405 (2001); W. Zhang, H. Pu, C. Search, and P. Meystre, *ibid.* **88**, 060401 (2002).

[15] S. Giovanazzi, D. O'Dell, and G. Kurizki, Phys. Rev. Lett. **88**, 130402 (2002); J. Phys. B **34**, 4757 (2001).

[16] D. O'Dell, S. Giovanazzi, G. Kurizki, and V.M. Akulin, Phys. Rev. Lett. **84**, 5687 (2000); S. Giovanazzi, D. O'Dell, and G. Kurizki, Phys. Rev. A **63**, 031603 (2001); S. Giovanazzi, G. Kurizki, I.E. Mazets, and S. Stringari, Europhys. Lett. **56**, 1 (2001); T.K. Ghosh, Phys. Rev. A **65**, 053616 (2002).

[17] J.D. Weinstein, R. deCarvalho, T. Guillet, B. Friedrich, and J.M. Doyle, Nature (London) **395**, 148 (1998); A. Fioretti, D. Comparat, A. Crubellier, O. Dulieu, F. Masnou-Seeuws, and P. Pillet, Phys. Rev. Lett. **80**, 4402 (1998); T. Takekoshi, B.M. Patterson, and R.J. Knize, *ibid.* **81**, 5105 (1998); A.N. Nikolov, E.E. Eyler, X.T. Wang, J. Li, H. Wang, W.C. Stwalley, and P.L. Gould, *ibid.* **82**, 703 (1999); H.L. Bethlem, G. Berden, and G. Meijer, *ibid.* **83**, 1558 (1999); A.N. Nikolov, J.R. Ensher, E.E. Eyler, H. Wang, W.C. Stwalley, and P. L Gould, *ibid.* **84**, 246 (2000); C. Gabbanini, A. Fioretti, A. Lucchesini, S. Gozzini, and M. Mazzoni, *ibid.* **84**, 2814 (2000); H.L. Bethlem, G. Berden, F.M.H. Crompvoets, R.T. Jongma, A.J.A. van Roij, and G. Meijer, Nature (London) **406**, 491 (2000); F.M.H.

Crompvoets, H.L. Bethlem, R.T. Jongma, and G. Meijer, *ibid.* **411**, 174 (2001).

[18] R. Wynar, R.S. Freeland, D.J. Han, C. Ryu, and D.J. Heinzen, Science **287**, 1016 (2000).

[19] J.D. Weinstein, R. deCarvalho, J. Kim, D. Patterson, B. Friedrich, and J.M. Doyle, Phys. Rev. A **57**, R3173 (1998).

[20] A.S. Bell, J. Stuhler, S. Locher, S. Hensler, J. Mlynek, and T. Pfau, Europhys. Lett. **45**, 156 (1999).

[21] C.C. Bradley, J.J. McClelland, W.R. Anderson, and R.J. Celotta, Phys. Rev. A **61**, 053407 (2000).

[22] J. Stuhler, P.O. Schmidt, S. Hensler, J. Werner, J. Mlynek, and T. Pfau, Phys. Rev. A **64**, 031405 (2001).

[23] J.D. Weinstein, R. deCarvalho, C.I. Hancox, and J.M. Doyle, Phys. Rev. A **65**, 021604 (2002).

[24] J. Kim, B. Friedrich, D.P. Katz, D. Patterson, J.D. Weinstein, R. DeCarvalho, and J.M. Doyle, Phys. Rev. Lett. **78**, 3665 (1997).

[25] S. Inouye, M.R. Andrews, J. Stenger, H.J. Miesner, D.M. Stamper-Kurn, and W. Ketterle, Nature (London) **392**, 151 (1998).

[26] J.L. Roberts, N.R. Claussen, S.L. Cornish, E.A. Donley, E.A. Cornell, and C.E. Wieman, Phys. Rev. Lett. **86**, 4211 (2001).

[27] M.D. Lukin, M. Fleischhauer, R. Côté, L.M. Duan, D. Jaksch, J.I. Cirac, and P. Zoller, Phys. Rev. Lett. **87**, 037901 (2001).

[28] D.S. Jin, J.R. Ensher, M.R. Matthews, C.E. Wieman, and E.A. Cornell, Phys. Rev. Lett. **77**, 420 (1996).

[29] M.-O. Mewes, M.R. Andrews, N.J. van Druten, D.M. Kurn, D.S. Durfee, C.G. Townsend, and W. Ketterle, Phys. Rev. Lett. **77**, 988 (1996).

[30] K.G. Singh and D.S. Rokhsar, Phys. Rev. Lett. **77**, 1667 (1996); M. Edwards, P.A. Ruprecht, K. Burnett, R.J. Dodd, and C.W. Clark, *ibid.* **77**, 1671 (1996); S. Stringari, *ibid.* **77**, 2360 (1996); L. You, W. Hoston, and M. Lewenstein, Phys. Rev. A **55**, R1581 (1997); P. Ohberg, E.L. Surkov, I. Tittonen, S. Stenholm, M. Wilkens, and G.V. Shlyapnikov, *ibid.* **56**, R3346 (1997).

[31] V.M. Pérez-García, H. Michinel, J.I. Cirac, M. Lewenstein, and P. Zoller, Phys. Rev. Lett. **77**, 5320 (1996).

[32] T. Bergeman, Phys. Rev. A **55**, 3658 (1997).

[33] C.J. Myatt, E.A. Burt, R.W. Ghrist, E.A. Cornell, and C.E. Wieman, Phys. Rev. Lett. **78**, 586 (1997); D.S. Hall, M.R. Matthews, J.R. Ensher, C.E. Wieman, and E.A. Cornell, *ibid.* **81**, 1539 (1998); D.S. Hall, M.R. Matthews, C.E. Wieman, and E.A. Cornell, *ibid.* **81**, 1543 (1998).

[34] D.M. Stamper-Kurn, M.R. Andrews, A.P. Chikkatur, S. Inouye, H.J. Miesner, J. Stenger, and W. Ketterle, Phys. Rev. Lett. **80**, 2027 (1998); J. Stenger, S. Inouye, D.M. Stamper-Kurn, H.J. Miesner, A.P. Chikkatur, and W. Ketterle, Nature (London) **396**, 345 (1998); H.J. Miesner, D.M. Stamper-Kurn, J. Stenger, S. Inouye, A.P. Chikkatur, and W. Ketterle, Phys. Rev. Lett. **82**, 2228 (1999).

[35] T.L. Ho and V.B. Shenoy, Phys. Rev. Lett. **77**, 3276 (1996); B.D. Esry, C.H. Greene, J.P. Burke, and J.L. Bohn, *ibid.* **78**, 3594 (1997); P. Öhberg and S. Stenholm, Phys. Rev. A **57**, 1272 (1998); E. Timmermans, Phys. Rev. Lett. **81**, 5718 (1998).

[36] M. Trippenbach, K. Góral, Y. Band, B. Malomed, and K. Rzążewski, J. Phys. B **33**, 4017 (2000).

[37] Th. Busch, J.I. Cirac, V.M. Pérez-García, and P. Zoller, Phys.

Rev. A **56**, 2978 (1997); B.D. Esry and C.H. Greene, *ibid.* **57**, 1265 (1998); P. Öhberg and S. Stenholm, J. Phys. B **32**, 1959 (1999).

[38] G. Meijer (private communication).

[39] T. Pfau (private communication).

[40] V.E. Zakharov, S.V. Manakov, S.P. Novikov, and L.V. Pitaevskii, *Teoria Solitonov: Metod Obratnoy Zadatchi* (Nauka, Moscow, 1980).

[41] E. Timmermans, R. Côté, and I. Simbotin, J. Phys. B **33**, 4157 (2000).

[42] P.A. Ruprecht, M. Edwards, K. Burnett, and C.W. Clark, Phys. Rev. A **54**, 4178 (1996).

[43] M. Brewczyk, K. Rzążewski, and C.W. Clark, Phys. Rev. A **57**, 488 (1998).